ARMY RESEARCH LABORATORY

Characterization of Cyclohexanone Inclusions in Class 1 RDX

by Rose A. Pesce-Rodriguez and Stephanie M. Piraino

ARL-TR-6962 June 2014

NOTICES

Disclaimers

The findings in this report are not to be construed as an official Department of the Army position unless so designated by other authorized documents.

Citation of manufacturer's or trade names does not constitute an official endorsement or approval of the use thereof.

Destroy this report when it is no longer needed. Do not return it to the originator.

Army Research Laboratory
Aberdeen Proving Ground, MD 21005

ARL-TR-6962 **June 2014**

Characterization of Cyclohexanone Inclusions in Class 1 RDX

Rose A. Pesce-Rodriguez and Stephanie M. Piraino
Weapons and Materials Research Directorate, ARL

REPORT DOCUMENTATION PAGE

Form Approved
OMB No. 0704-0188

1. **REPORT DATE** *(DD-MM-YYYY)*	**2. REPORT TYPE**	**3. DATES COVERED (From - To)**
June 2014	Final	12/2012 to 6/2013

4. TITLE AND SUBTITLE
Characterization of Cyclohexanone Inclusions in Class 1 RDX

5a. CONTRACT NUMBER

5b. GRANT NUMBER

5c. PROGRAM ELEMENT NUMBER

6. AUTHOR(S)
Rose A. Pesce-Rodriguez and Stephanie M. Piraino

5d. PROJECT NUMBER

5e. TASK NUMBER

5f. WORK UNIT NUMBER

7. PERFORMING ORGANIZATION NAME(S) AND ADDRESS(ES)
U.S. Army Research Laboratory
ATTN: RDRL-WML-B
Aberdeen Proving Ground, MD 21005

8. PERFORMING ORGANIZATION REPORT NUMBER
ARL-TR-6962

9. SPONSORING/MONITORING AGENCY NAME(S) AND ADDRESS(ES)

10. SPONSOR/MONITOR'S ACRONYM(S)

11. SPONSOR/MONITOR'S REPORT NUMBER(S)

12. DISTRIBUTION/AVAILABILITY STATEMENT
Approved for public release; distribution unlimited.

13. SUPPLEMENTARY NOTES

14. ABSTRACT
Neat Class 1 RDX and Class 1 RDX from prills and pressed Comp A-3 (type II) have been characterized with respect to solvent inclusions in support of a U.S. Army Research Laboratory (ARL) program to model Multiscale Response of Energetic Materials (MREM). It was observed that even "dry" RDX retains surface-adsorbed solvent and the level of this adsorbed solvent can be reduced, but not eliminated, by heating at 50 °C under vacuum. Such treatment does not remove included solvent unless the temperature is high enough to cause the included solvent to expand sufficiently to result in micro-cracks. Desorption gas chromatography (GC)-mass spectrometry (MS) was used to quickly estimate both the average volume and weight percent of RDX solvent inclusions. Included solvent in Class 1 RDX accounts for less than 0.04% of total mass, whereas adsorbed solvent accounts for about half that. The average inclusion size for Class 1 RDX was estimated to be ~1 μm. Pressing Comp A-3 prills into charges results in particle size reduction and loss of solvent inclusions. It is proposed that solvent liberated from inclusions can aid in binder-filler interaction in the pressed sample by solvating material at interfaces and, perhaps, by smoothing sharp edges resulting from cracked particles.

15. SUBJECT TERMS
RDX, cyclohexanone, inclusions, voids, Comp A-3, residual solvent

16. SECURITY CLASSIFICATION OF:			**17. LIMITATION OF ABSTRACT**	**18. NUMBER OF PAGES**	**19a. NAME OF RESPONSIBLE PERSON**
a. REPORT	**b. ABSTRACT**	**c. THIS PAGE**			Rose A. Pesce-Rodriguez
Unclassified	Unclassified	Unclassified	UU	30	**19b. TELEPHONE NUMBER** (*Include area code*) (401) 306-1877

Contents

List of Figures

List of Tables

Acknowledgments

The authors would like to acknowledge Dr. Brian Alexander (BAE Systems) for information on RDX particle size and processing; Dr. Scott Kucuck for providing a 3-in Comp A-3 Billet; and Dr. Brian Roos for pressed Comp A-3 billets. We would also like to thank Dr. Betsy Rice, Dr. John Brennan, Dr. DeCarlos Taylor and Dr. Josh Moore (U.S. Army Research Laboratory [ARL]) for discussions regarding compositional information pertinent to their modeling effort under the Multiscale Response of Energetic Materials (MREM) program, and the Weapons and Materials Research Directorate, Lethality Division for financial support for this work.

INTENTIONALLY LEFT BLANK.

1. Background

The effort in this work is a continuation of that reported in reference 1 and focuses on providing experimental data in support of a U.S. Army Research Laboratory (ARL) initiative called "Multiscale Modeling of Energetic Materials" (MREM). The MREM program aims, for the first time, to model an explosive formulation from the atomic to continuum scales, with the ultimate objective of modeling and predicting explosive sensitivity response. In such a major undertaking, it is natural to choose to model as simple a system as possible. A logical choice is Comp A-3, whose formulation is often given as "91% RDX, 9% polyethylene." As described in reference 1, the actual formulation is a bit more complicated. Additional materials present in the formulation include trace levels of emulsification agents, a non-trivial amount of HMX, and residual solvent used in the purification and recrystallization of RDX. The characterization of this solvent impurity and its implications for RDX crystal morphology and behavior in Comp A-3 is the focus of this investigation.

One of the earliest literature reports on RDX inclusions was by Gross in 1970 (*2*). Gross contrasted the growth of liquid-filled inclusions in RDX with the growth of gas-filled inclusions in alkali halides as reported by Amelinckx (*3*) and noted that gas-filled cavities can grow more easily than liquid-filled cavities because gases can diffuse more easily. Gross noted that RDX inclusions appeared to grow when a crystal with existing inclusions was subjected to photolytic degradation, and indicated that these inclusions contained decomposition gases and grew in size as photolysis progressed. Borne, Patedoye, and Spyckerelle (*4*) found RDX inclusions to contain air, water, and crystallization solvent (acetone or cyclohexanone). The authors also presented data for analysis of air, water, and residual solvent (acetone and cyclohexanone) for samples with densities ranging from 1.769 to 1.799 g/cm^3. They observed an inverse relationship between density and the levels of included air, water, and solvent. Batten (*5*) reported on three types of solvent impurity in RDX: "weakly held," i.e., removed by vacuum at ambient temperature; "strongly held," i.e., removed by vacuum at heat (160 °C); and "tenaciously held," i.e., removed by sublimation/trapping of RDX. Based on results to be presented herein, we would describe the first type as "loosely" adsorbed solvent (more than a monolayer) on exterior surfaces of particles; the second type as likely a monolayer of surface adsorbed solvent that is very difficult to remove except by temperatures high enough to result in RDX sublimation, and possibly, loss of included solvent; and the third type as included solvent.

A report by Sharma et al. (*6*) examined the interior of RDX inclusions by atomic force microscopy (AFM). They cleaved laboratory-grown crystals along the {001} plane to provide a cross-sectional view of the inclusions. The authors described the inclusions as "nano-caverns, ranging in size from 10 nm to a few microns, with very complicated shapes and tentacle-like arms." At the outside borders of the inclusions, the authors noted white deposits that were

20–200 nm in size, which were attributed to evaporated solvent, presumably having recrystallized RDX with which it came in contact, and also "complicated porous defects, having large surface-to-volume ratios and fine cracks and tentacles running out of them." The authors speculated that the fine cracks might not be conducive to the development of hot spots from adiabatic compression, as they would tend to allow gases to leak away. It was further speculated that inclusion shape might change as a result of dissolution and recrystallization caused by seasonal and diurnal temperature cycling. In a very recent work, Bouma, Duvalois, and van der Heijden (*7*) performed microscopic analysis of three reduced-sensitivity RDX (RS-RDX) samples with different shock sensitivities that were first embedded in an epoxy resin and then cross-sectioned. The authors documented growth bands, growth sectors, and defects that are aligned with the crystallographic structure. Different types of defects were found to be specific for each of the RDX samples. Inclusions as small as 0.5 μm were observed.

Analysis of a series of RS-RDX samples was performed by small angle neutron scattering (SANS) and ultra small angle neutron scattering (USANS) by Stolz, Mason, and Hooper (*8*). The RDX was prescreened to select only particles with a mean particle size of 200 ± 20 μm. The authors reported that HMX content was determined for all samples and found to be significant in just one sample (3.83% in the sample from Ordnance Systems, Inc., that had been manufactured by the Bachman process). The authors also reported that nuclear magnetic resonance (NMR) analysis of all samples found no solvent impurity (within a limit of detection of <1% volume fraction) in any RS-RDX sample, but confirmed that they could detect solvent in freshly recrystallized RDX. This was interpreted to mean that solvent had diffused out of the reduced sensitivity RDX and that any inclusions in the particles contained only gas; the authors suggest that the inclusions are filled with air. SANS/USANS analysis revealed internal fractal surfaces ranging in length from ~50 nm up to ~20 μm, and observed that the volume fraction of inclusions smaller than 20 μm tracked well with sensitivity testing of the materials. Based on the assumption that cavities are filled with air, the authors estimated an inclusion volume fraction between 0.004% and 0.115%.

Another group, ter Horst et al. (*9*), provide a possible explanation for the origins of inclusions in RDX and the observation that inclusions don't occur in RDX crystallized in cyclohexanone saturated with water. The basis of the explanation is that a condensation product of cyclohexanone and an RDX impurity ("TAX", i.e., 1(N)-acetyl-3,5-dinitro-1,3,5-triazine) blocks the normal placement of RDX molecules in the crystal lattice and forces the lattice to form around the hindrance caused by the adduct, resulting in an inclusion. By pre-saturating cyclohexanone with water, the equilibrium is shifted away from the cyclohexanone-TAX condensation product, thereby avoiding the formation of inclusions. Another method to avoid the production of inclusions is offered by Stolz et al. (*10*). The group produced crystals with very few inclusions and improved sensitivity with a combination of sonication and control of the solvent evaporation rate. The proposed explanation for their success is the ability to induce nucleation at low supersaturation levels. The method also results in particles with a uniform

crystallite morphology and narrow particle size. Kim et al. (*11*) explored the effect of supersaturation in various solvents on the degree of inclusion formation. They reported that supersaturation increases with increasing cooling rate for all solvents studied (cyclohexanone, acetone, N-methylpyrrolidone, dimethylsulfoxide, and γ-butyrolactone). The authors found that acetone and cyclohexanone required a low degree of supersaturation to avoid formation of inclusions, while N-methylpyrrolidone and dimethylsulfoxide fared better with a high degree of supersaturation.

Czerski and Proud (*12*) found that RDX shock sensitivity (as measured by the gap test) was correlated not with inclusions, but with the presence of surface dimples on small crystals (10–30 μm) and with angularity of large crystals (100–300 μm), as a result of viscoplastic heating at sharp corners that contact neighboring crystals. Borne and Beaucamp (*13*) and Borne and Ritter (*14*) found that there was a correlation between solvent inclusions and the shock sensitivity of the formulation, although they also found deviations to the correlation. Doherty and Watt (*15*) reported that less sensitive RDX tended to have fewer small internal defects ("cloudy areas" that are a collection of very small inclusions) than more sensitive RDX, but also concluded that internal defects alone were not sufficient to predict the sensitivity of RDX crystals.

There are many reports that address the effects of process-induced damage to RDX crystals. Lochert, Franson, and Hamshere (*16*) reported on RS-RDX in RDX/polyethylene wax compositions. This is of interest to us because of the similarity to Comp A-3. The authors reported that the shock sensitivity of pressed compositions increases as the density increases, presumably as a result of damaging RDX crystals under the load required to obtain the higher densities, thereby negating the shock sensitivity benefits of using a RS-RDX. Lochert, Franson, and Hamshere also note that at lower densities, RS-RDX in pressed compositions is thought to be undamaged and demonstrates reduced shock sensitivity. Consistent with the findings by Lochert, Franson, and Hamshere are the results by Wilson (*17*), who found that the shock sensitivity of compacted RDX/polyethylene explosive increases with increasing density. However, Borne, Mory, and Schlesser (*18*) reported that pressing of 70 wt.% RS-RDX with 30 wt.% wax does not result in crystal fracture. This conclusion was inferred from sensitivity measurements, not microscopic examination. Addiss and Proud (*19*) conducted compaction studies on RDX using either Instron or drop-weight testing. The Instron tests were carried out at a relatively slow rate (4 mm/min), which reportedly gave the RDX particles time to rearrange themselves into an "equilibrium arrangement," whereas the drop-weight test would have compressed the crystals at a much faster rate (3 m/s) and resulted in crystals getting hung up on each other before fracturing. Despite the different compaction mechanisms used, the outcome was nearly identical. Under both conditions, particles were reduced in size from 1200 μm to 400–500 μm. The authors found no obvious correlations between the resistance to compaction and the sensitivity. A study of RDX compression by cone-beam micro-computed tomography, a non-destructive technique, was conducted by Zhang et al. (*20*), and showed that fracture is

strongly influenced by applied pressure and the shape of the crystal mold and that crack direction was roughly perpendicular to confinement forces by neighbor crystals. Zhang et al. report that crack propagation usually started at inclusions.

2. Experimental

A Zeiss Stemi 2000-C optical microscope equipped with a digital camera was used to capture images of the tested samples using AxioVision software (Release 4.8.1).

Analysis of desorbable species was performed using an Agilent gas chromatography (GC)-mass spectroscopy (MS) (Model 6890N GC and Model 5973N MSD) system fitted with a Pyroprobe 2000 (CDS Analytical, Oxford, PA). The GC column used was a HP-5 capillary column (0.25 mm × 30 m, 0.25-mm film). The injector temperature was 200 °C and the Pyroprobe interface temperature was 175 °C. The GC oven temperature program was as follows: 50 °C isothermal for 1 min, 50–250 °C at 40 °C/min, and 250 °C isothermal for 1 min. The Pyroprobe was programmed to give a 20-s desorption pulse at 175 °C (heating rate 1000 °C/s). The sample was held within the coil of the Pyroprobe by first placing it in a quartz tube containing a small plug of glass wool and then inserting the entire tube into the coil.

Samples analyzed include Class 1 RDX, which is defined as RDX with the particle size distribution given in table 1. Figure 1 gives typical particle size distributions for RDX used in Comp A-3 (*21*). The nominal particle size of such a distribution is approximately 200 μm.

Also analyzed in this work were “small” Comp A-3 billets (1 cm; L/D=1) and prepared as indicated in table 2, as well as a larger billet (3-inch; L/D=1).

Table 1. Granulation requirement for Class 1 RDX.

Through U.S. Standard Sieve Number	**Sieve Opening (μm)**	**Weight %**
20	850	100–96
50	300	100–90
100	150	90–30
200	75	46–20

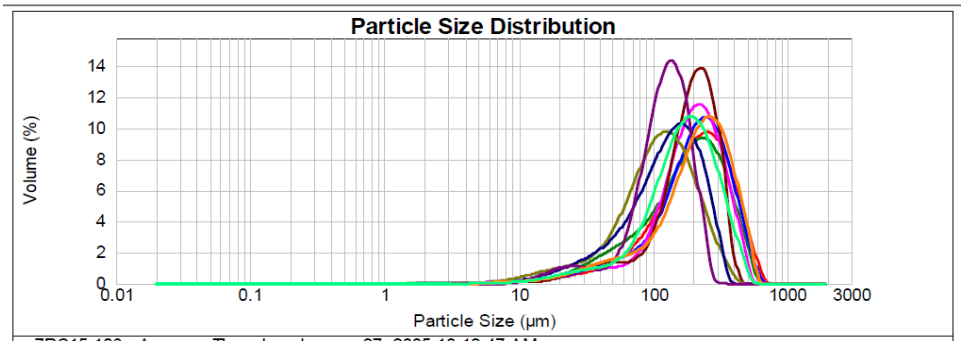

Figure 1. Particle size distribution for Class 1 RDX typically used in Comp A-3 Type II (*21*).

Table 2. Applied pressure and resulting densities for Comp A-3 billets (*22*).

Applied Pressure (psi)	Resulting Density (g/cc)
2,500	1.55
8,200	1.61
62,000	1.64

3. Results and Discussion

3.1 Characterization of Inclusions:

Optical micrographs of as-received and thermally treated Class 1 RDX are given in figure 2. The as-received RDX has obvious inclusions resulting in a slightly "cloudy" appearance. The largest particles appear to be on the order of 350 µm. After thermal treatment, the RDX particles still appear to have inclusions and the largest particles still appear to be on the order of 350 µm. The main difference between the as-received and thermally treated samples is the increased cloudiness in the latter. This cloudiness is more readily seen in figure 3, which shows an RDX crystal grown from acetone. The photo on the left was taken before thermal treatment and the photo on the right after desorption (D)-GC-MS analysis at 175 °C. Several interesting observations may be made. The samples themselves were observed to change from clear to opaque), and the chromatogram from the resulting D-GC-MS analysis (figure 4, top) indicated a number of small peaks that were identified as acetone, the recrystallization solvent. These acetone peaks were more readily observed when a selected ion chromatogram (SIC, m/z= 43) was obtained (figure 4, bottom). It is assumed that each peak in the chromatogram corresponded to the release of solvent from one or more inclusions. If the solvent had been adsorbed at the surface, or come from just one large inclusion, only one peak would have been observed. The fact that there were several peaks means there had to be at least that number of inclusion. Furthermore, it appears that the solvent "eruptions" resulted in micro-cracks in the crystal,

resulting in the hazy appearance. Re-analysis of the thermally-treated sample by D-GC-MS indicated that the sample had lost all trace of residual solvent.

Based on our analysis of the crystal grown from acetone, it was concluded that D-GC-MS is a useful tool for analyzing fluid or gas inclusions in crystals and could be used not only to identify the contents of the inclusion, but also to estimate the volume of solvent trapped in the inclusions, and therefore, the volume of the inclusions themselves. Such information is critical to the MREM effort and was therefore applied to Class 1 RDX used in Comp A-3. Since the solvent used in the preparation of the Class 1 RDX was not acetone, but cyclohexanone, the selected ion chromatogram (SIC) was obtained using m/z = 98. Figure 5 gives the mass spectrum of cyclohexanone compared with mass spectrum obtained from Class 1 RDX and indicates the m/z=98 peak in both. There are obviously many other m/z values that could have been used to identify cyclohexanone eruptions; m/z=98 was selected because it worked well to identify cyclohexanone in both Class 1 RDX and Comp A-3, which gives a very complicated chromatogram because of its more complex composition.

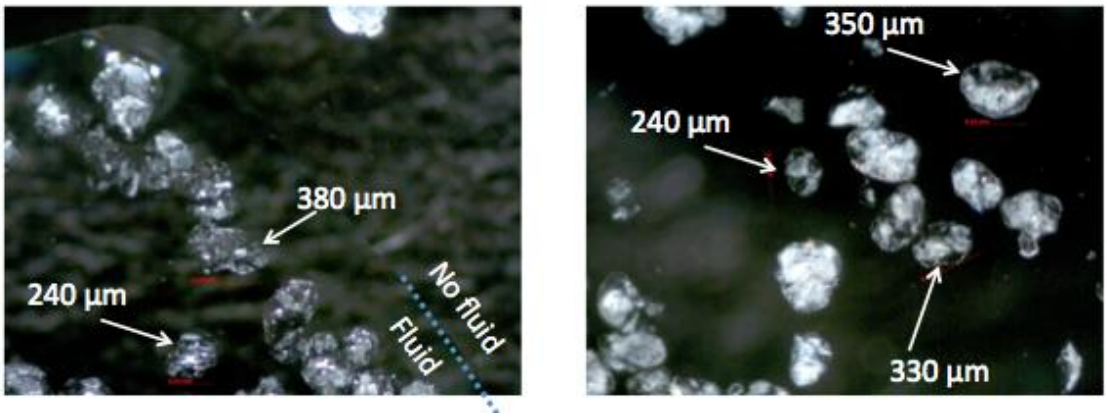

Figure 2. RDX optical micrographs (both in fluid with refractive index=1.6). Left: Class 1 RDX, as-received and right: Class 1 RDX after thermal desorption.

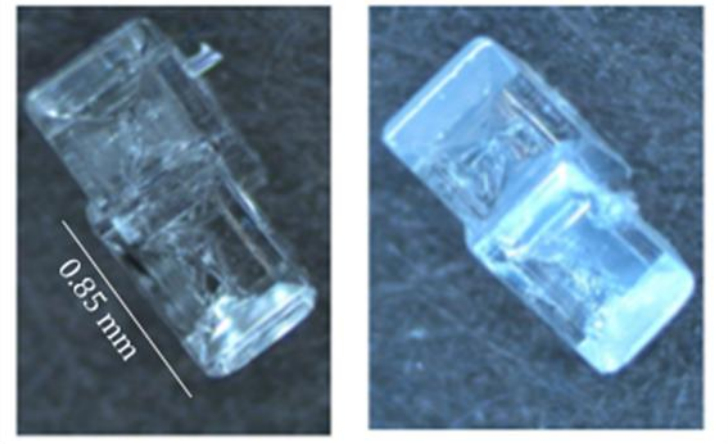

Figure 3. RDX recrystallized from acetone. Left: before thermal treatment and right: after thermal treatment.

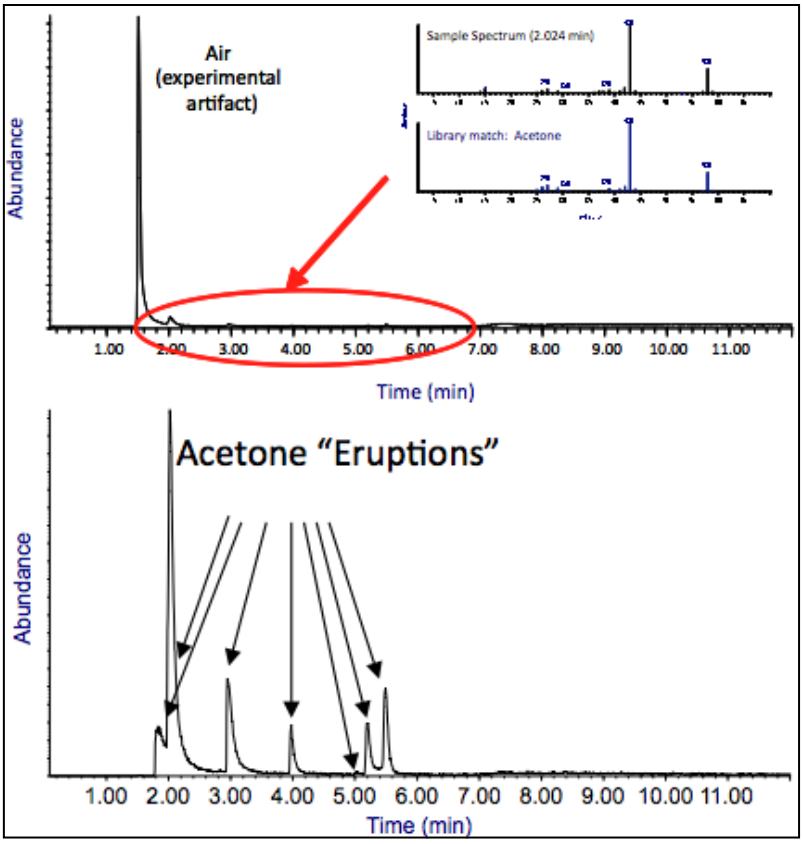

Figure 4. D-GC-MS result for RDX crystal heated at 175 °C. Top: Total ion chromatogram (with library match) and bottom: Selected ion chromatogram [m/z=43 (acetone)].

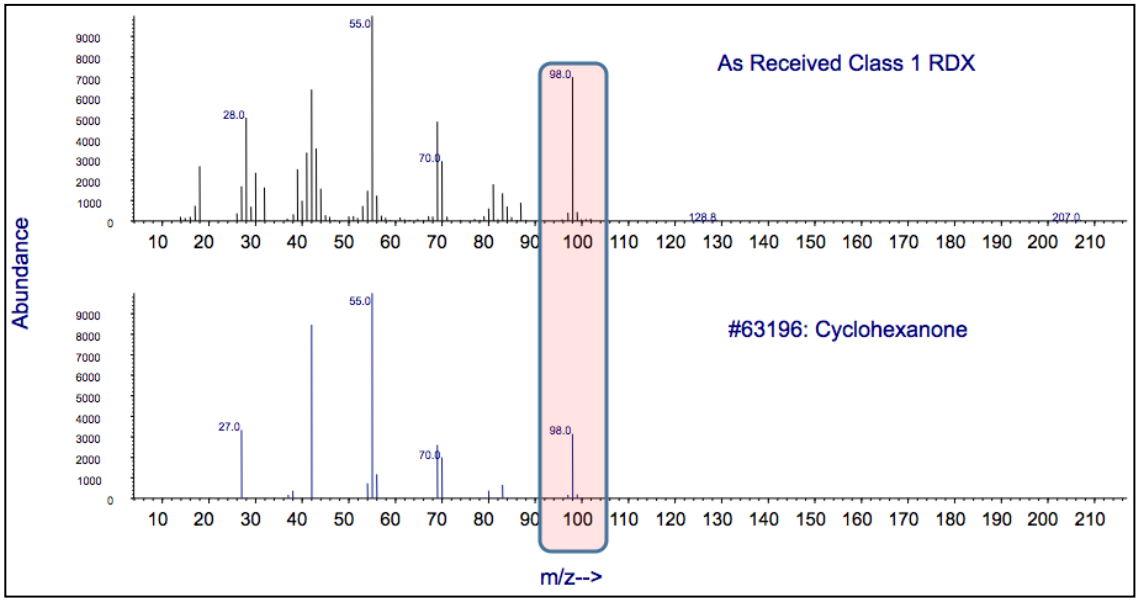

Figure 5. Top: Mass spectrum of RDX peak and bottom: library match (m/z = 98 is selected for tracking cyclohexanone in Class 1 RDX in figure 6).

Results of the D-GC-MS analysis of Class 1 RDX are given in figure 6 and revealed approximately 140 peaks confirmed by GC-MS analysis to be from cyclohexanone. In disagreement with Borne, Patedoye, and Spyckerelle (*4*), no air or water was found in the inclusions. The sample was collected after the analysis, observed by optical microscopy, and found to be comprised of approximately 170 particles, each with many apparent inclusions. Based on this information, it was concluded that each peak must correspond to the "eruption" of more than one inclusion, and likely from more than one particle at a time.

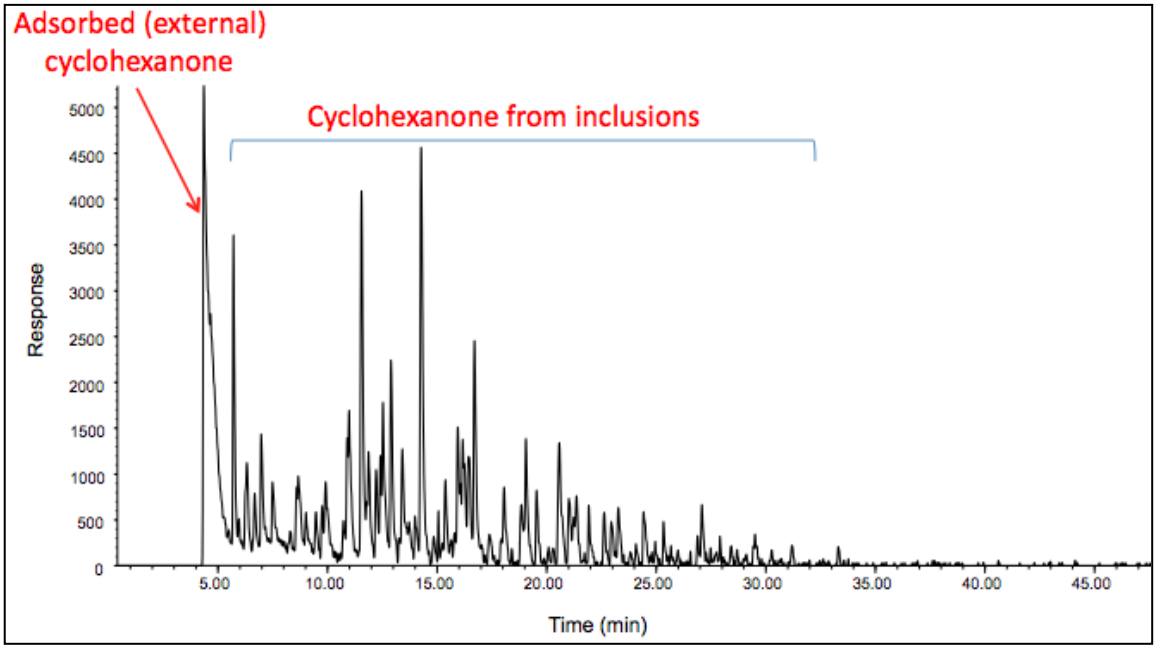

Figure 6. Selected ion chromatogram (SIC, m/z=98, cyclohexanone) for RDX desorption at 175 °C.

All but the very smallest of these peaks were integrated and converted to volume of cyclohexanone in µL and μm^3 based on cyclohexanone's known density (0.9478 g/mL) and the simplifying assumption that a single peak come from a single inclusion. Figure 7 gives a graphical representation of the results. The two plots differ only by the units of the *y*-axis. The average inclusion volume assuming one inclusion per peak was calculated to be approximately 7.7E-06 µL or 7600 μm^3, which is equivalent to a sphere with a diameter of approximately 12.2 µm. Optical microscopic inspection of a large number of Class 1 RDX crystals indicates that most crystals have several inclusions that are tens of microns in size, as well as hundreds of inclusions that are on the scale of tenths of microns or smaller. Assuming anywhere from 10 to 100 inclusions per crystal would result in an estimated average inclusion size of 100–1 µm. The total included cyclohexanone was found to account for approximately 0.070% of total sample volume and 0.035% of total sample mass. Adsorbed cyclohexanone, which we observe in the first peak in the chromatogram, accounts for ~0.02% of total sample volume and ~0.01% of total sample mass. Note that the density of RDX is about twice that of cyclohexanone (1.82 vs. 0.95 g/cm^3).

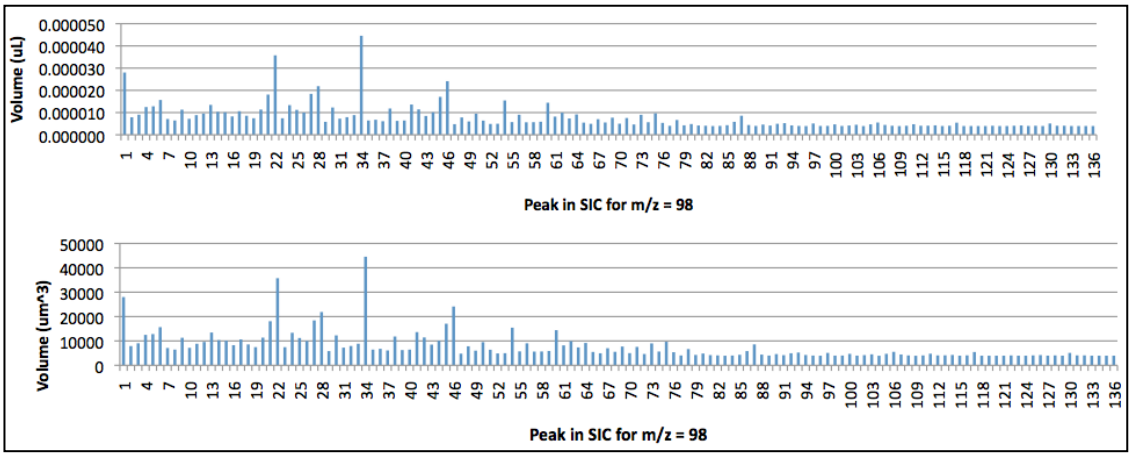

Figure 7. Calculated volumes of cyclohexanone required to generate each inclusion peak.

Comparison of the results for average inclusion size described in the preceding paragraph with those of Stolz et al. (*8*) indicates reasonable agreement. Based on SANS analysis, Stolz et al. concluded that inclusions accounted for between 0.004% and 0.115% of total sample volume (compared with the ARL estimate of 0.070%). Also van der Heijden and Bouma (*23*) inferred inclusion volumes for HMX by comparison of measured and theoretical densities and found a "bad" batch with a density of 1.900 g/cm^3 to have 0.16 vol.% inclusions and a "good" batch with a density of 1.902 g/cm^3 to have 0.05 vol.% inclusions. The ARL estimate of 0.02 vol.% for RDX is certainly in line with the values for HMX inferred by van der Heijden and Bouma. Stolz et al. (*8*) reported the absence of included solvent in RS-RDX. Their results are consistent with the ARL estimate of 0.035 wt.%, given that their limit of detection was 1 wt.%. Regarding estimated inclusion size, a value of approximately 0.1–1 μm average size (assuming spherical geometry) is reported herein for Class 1 RDX; Stolz et al. estimate 60 nm to 20 μm for RS-RDX, again in reasonable agreement. While Stolz et al. reported that while they could not detect solvent in RDX inclusions in RS-RDX, they could detect solvent in freshly recrystallized RDX, and postulated that absence of solvent in the RS-RDX might be the result of diffusion of the solvent from the crystals. We suggest that it is not likely that this happened given that D-GC-MS analysis indicates that solvent is still present in Class 1 RDX even after it had been heated at 50 °C under vacuum for 3 h. The more likely explanation for the apparent absence of solvent in the reduced sensitivity samples examined by Stolz et al. is that the solvent content was simply below their limit of detection. Considering data of Czerski and Proud (*12*), we would expect solvent levels in RDX with the densities of the Stolz et al. samples (i.e., 1.785 g/cm^3) to be quite low, i.e., on the order of 0.03 wt.%. If this were the case, then the solvent level would clearly have been below the limit of detection for the NMR analysis that was performed. But what if Stolz et al. were right and solvent did diffuse away? To help address this issue, one might consider the findings of Waldschmidt et al. (*24*), who examined solvent inclusions in non-energetic organic crystals that were 30 years old. Among the findings were that included solvent did not diffuse away from the crystals, but that the inclusion shapes had evolved toward that of

"negative crystals," i.e., of cavities bounded by crystallographic faces (*25, 26*). For example, benzoyl lusitanicol normally crystallizes into needles and was found by Waldschmidt et al. to demonstrate elongated "needle like" solvent-filled inclusions that sometimes included a gas bubble. Waldschmidt et al. observed that gas bubbles would disappear if the crystal were heated to 55 °C, and then reappear when cooled to room temperature. They did not analyze the composition of the bubble, but clearly the gas in the bubble was composed either of solvent vapor or something soluble in the solvent. The authors also observed that the size of the inclusions increased slightly with increasing temperature (presumably as a result of swelling of the included solvent), and then reverted to its original size on cooling. As it turns out, the phenomenon of gas bubble disappearance/reappearance that Waldschmidt et al. reported is not new and has been used for decades by the geology community to estimate the temperature at which crystal inclusions formed (*26, 27*).

Given that liquids are known to generally have larger coefficients of thermal expansion than solids, and that RDX samples analyzed by ARL were heated at 175 °C (not 55 °C as in Waldschmidt et al.), it is completely reasonable to assume that included solvent expanded sufficiently to generate micro-cracks in the RDX crystals when heated to that temperature, thereby allowing solvent to escape and resulting in the observed haziness of the crystals after thermal treatment. In the absence of such a significant thermal treatment, solvent inclusions in RDX crystals are presumed to be unlikely to "dry up."

As for the significance of "negative crystals" with respect to the inclusions observed in RDX, the concept is consistent with the observations by Bouma et al. (*7*), who reported that RDX defects (including fluid-filled inclusions) tended to be aligned with crystallographic orientation. Figure 8 shows an ARL optical micrograph of a Class 1 RDX particle showing what might be a tendency toward alignment of defects in two lobes of a crystal. Class 1 RDX particles generally have so many defects that it is difficult to say that the apparent alignment is not more than a coincidence. When observed on a very small scale (i.e., RDX dendrites with widths on the order of tens of microns), large internal defects that might be considered to be inclusions were observed by Duan et al. (*29*) and provide additional evidence of the tendency of RDX defects to conform to crystallographic features. Given the apparent agreement between reports by the authors cited here, it is proposed that as RDX crystals age, inclusions are likely to assume shapes and orientations that are increasingly consistent with crystal orientation. As proposed by Sharma et al. (*6*), inclusion shape may in fact change as a result dissolution and recrystallization caused by seasonal and diurnal temperature cycling. So long as crystals are not subjected to temperatures that are sufficiently high as to excessively swell residual solvent and cause micro/nano fissures in the crystal, RDX will continually go through a cycle of dissolution and crystal growth consistent with crystal orientation without concomitant loss of solvent.

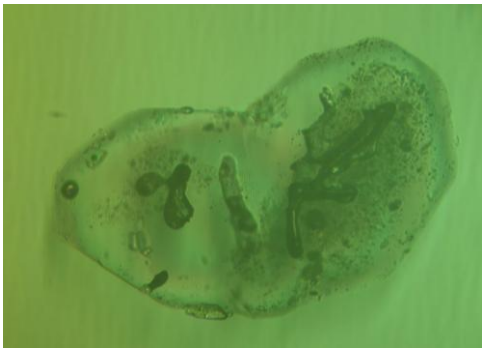

Figure 8. Optical micrograph of a Class 1 RDX particle (in RI matching fluid).

3.2 Effect of Pressure on Inclusions

D-GC-MS results allow us to distinguish between solvent trapped in inclusions and solvent adsorbed on the surface of the crystal. Adsorbed solvent desorbs relatively easily when crystals are heated at 175 °C and appear in the first peak in the gas chromatogram. Included solvent must first expand and generate micro-cracks in the crystal before diffusing away from the crystal. Figure 9 shows the SICs (m/z = 98) for Class 1 RDX and a sample taken from a Comp A-3 billet. It is observed that relative to Class 1 RDX, the interfacial cyclohexanone in the Comp A-3 billet increases slightly and the included cyclohexanone disappears. The proposed explanation for this observation is that during the pressing process, RDX crystals crack and liberate trapped solvent that either flows to the original exterior surface of the crystal or remains in place on what becomes a new exterior surface in the cracked crystal. The fact that included solvent transitions to surface-adsorbed solvent when crystals or prills are pressed can work in favor of reduced sensitivity by being available for recrystallization of newly exposed sharp surfaces and also for improved interaction with binder by solvating material at interfaces. As reported in reference 1, cyclohexanone interacts well with both RDX and oxidized polyethylene, suggesting that surface-adsorbed solvent will aid in binder-filler interaction.

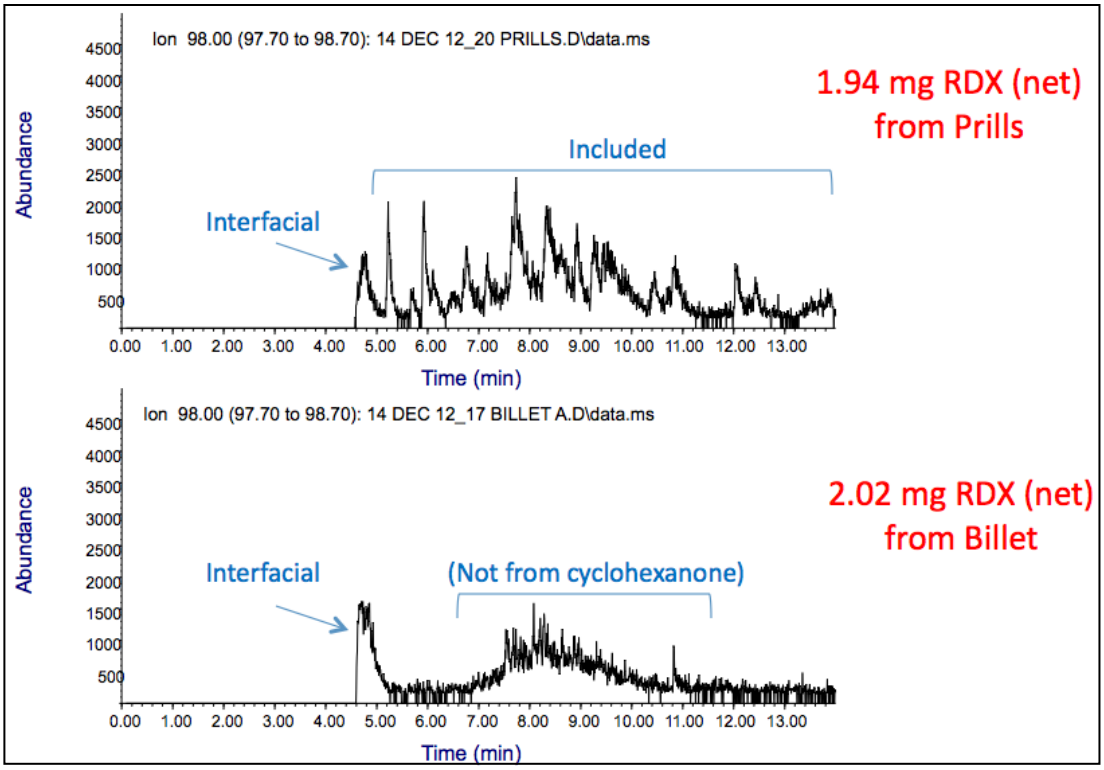

Figure 9. SICs (m/z = 98) for Class 1 RDX (top) and Comp A-3 billet (bottom).

To confirm the hypothesis that included solvent decreases in pressed samples, particles from Comp A-3 prills and pressed billets were analyzed. Figure 10 shows micrographs of Comp A-3 prills and a 1-cm billet that has been "deconsolidated" by gently picking them apart with fine dental tools. It is observed that the largest particles from the prills (figure 10, left) are on the order of 300 µm (normal for Class 1 RDX), and that there are relatively few small particles as compared with the deconsolidated billet (figure 10, right), which has many small, non-spherical particles. It is proposed that these small particles are RDX fragments produced during the pressing process. Such particle size reductions has been reported for Comp A-3 in a 5-in/54 charge (*30*), where it was observed that particles were reduced from 185 to 140 µm (Class A to Class G). (A comparison of the particle sizes in these classes is given in table 3.) Figure 11 shows particles from a larger Comp A-3 billet (3-in/7.62-cm with L/D = 1). No particles larger than 250 µm were observed for this sample, whereas many small, non-spherical particles were observed.

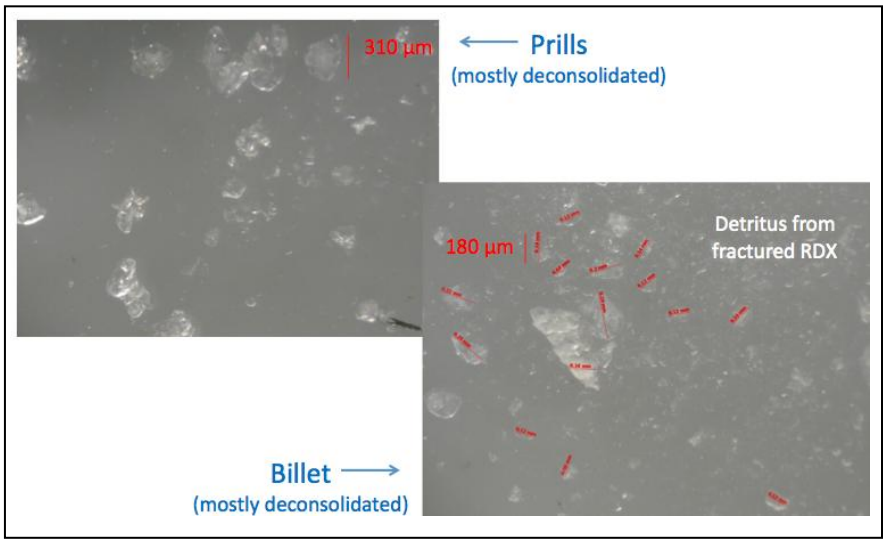

Figure 10. Optical micrographs of Comp A-3 (in RI matching fluid). Left: deconsolidate prills and right: deconsolidated 1-cm billet.

Table 3. Granulation requirement for Class 1, A and G RDX (*31*).

Through U.S. Standard Sieve Number	**Sieve Opening (µm)**	**Weight-% - Class**		
		1	**A**	**G**
20	850	100–96	98	–
50	300	100–90	90	98
100	150	90–30	60	90
200	75	46–20	25	46

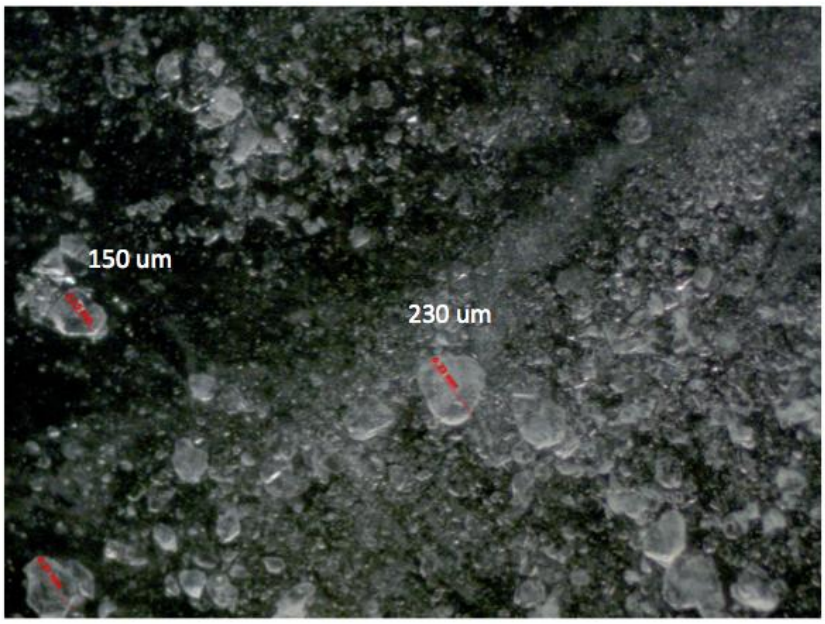

Figure 11. Optical micrograph of deconsolidated 3-inch Comp A-3 (in silicone oil).

Samples taken from the center and edge of the 3-in billet (figure 12) were also examined by D-GC-MS. Results are shown in figure 13 and indicate only surface-adsorbed cyclohexanone (no included solvent). This is consistent with observations from the 1-cm billet. Mass spectra associated with the peaks between 5 and 11 min in figure 13 are hydrocarbons from the oxidized polyethylene binder, not cyclohexanone.

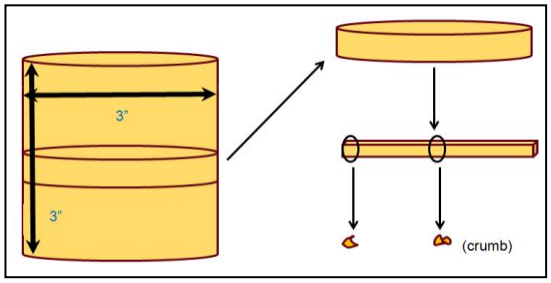

Figure 12. Sampling locations for 3-in Comp A-3 charge.

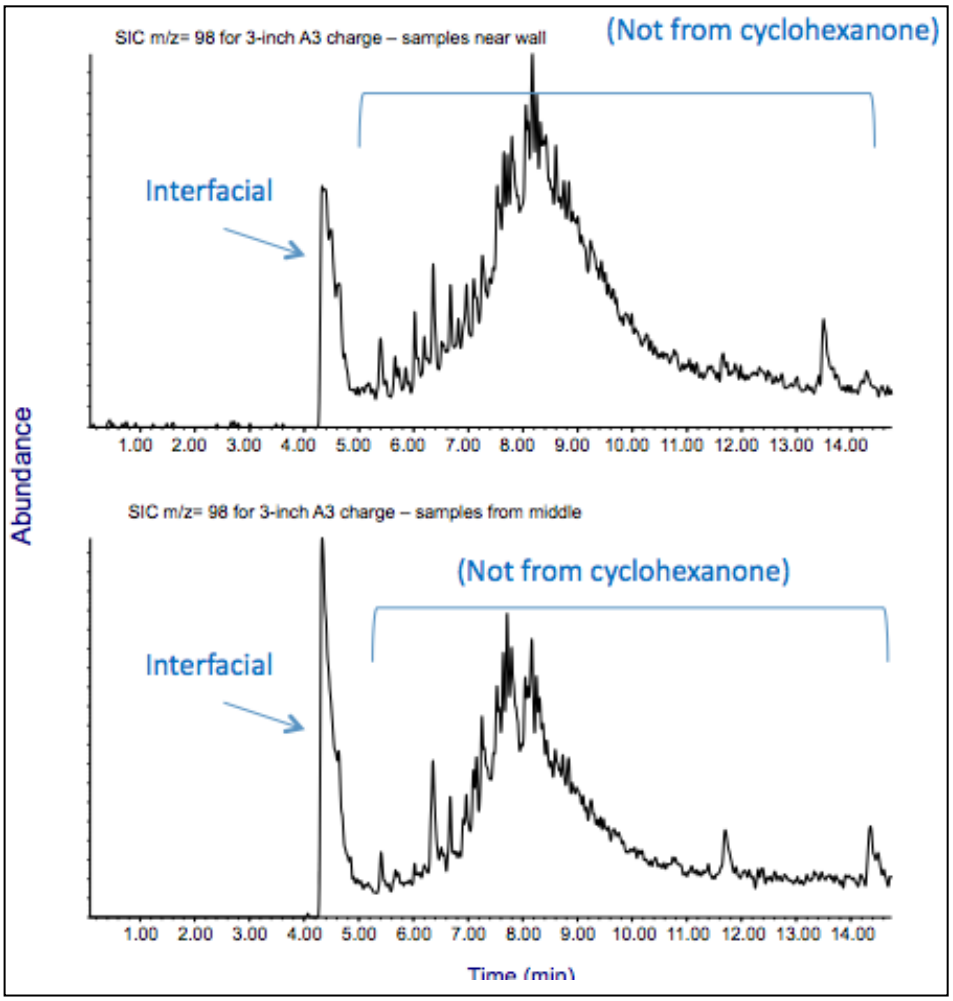

Figure 13. D-GC-MS analysis of 3-in Comp A-3 charge. Top: sampled near wall (as indicated in figure 12) and bottom: Samples from middle (as indicated in figure 12).

Results regarding RDX particle size reduction as a result of pressing are consistent with reports by Addiss and Proud (*19*) and Zhang et al. (*20*), but inconsistent with results by Borne, Mory, and Schlesser (*18*). The discrepancy likely arises from the fact that Addis and Proud and Zhang et al. analyzed bare RDX crystals, but Borne et al. studied RDX with 30 wt.% wax binder. Comp A-3, with 9 wt.% oxidized polyethylene binder and poor coverage of filler, would be expected to be somewhere in between, but clearly responds more like bare RDX than RDX coated with a relatively large amount of binder. Reports on the increase in sensitivity on pressing as reported by Lochert et al. (*15*) and Wilson (*16*) suggest that modelers intending to predict RDX sensitivity should pay careful attention to the effect of processing on RDX morphology. These effects include particle size reduction, particle shape changes (including sharp, broken edges), loss of most solvent inclusions, and possibly improved binder-filler interactions (as a result of liberation of included solvent that can solvate material at interfaces).

4. Conclusions

The following are the results of our study:

- For the first time, it was determination that cyclohexanone is present not only in RDX crystals as inclusions, but also adsorbed on the surface.
- Moderate heating (50 °C) of RDX under vacuum can reduce (but not eliminate) surface adsorbed cyclohexanone, but not included cyclohexanone.
- D-GC-MS has been shown to give quick and reliable estimates of average inclusion size, volume, and composition.
- The average inclusion size in class 1 RDX was estimated to be approximately 1 μm.
- Total included cyclohexanone accounts for the following:
    - ~0.070 % of total sample volume
    - ~0.035 % of total sample mass
- Adsorbed cyclohexanone accounts for the following:
    - ~0.02 % of total sample volume
    - ~0.01 % of total sample mass
- On pressing of Comp A-3 billets to densities appropriate for field use:
    - RDX particle size is reduced.
    - Interfacial (binder/RDX) cyclohexanone increases.

    - Included cyclohexanone disappears.
- The loss of included solvent and reduction of RDX particle size was also found to occur in large (3-in) Comp A-3 billets, suggesting that observed effects are not (charge) size dependent.

5. References

1. Pesce-Rodriguez, R. A.; Piraino, S. M. *Chemical and Physical Characterization of Comp A-3 Type II Prills*; ARL-TR-6498; U.S. Army Research Laboratory: Adelphi, MD, June 2013.
2. Gross, K. A. Liquid Inclusions in RDX Crystals. *Journal of Crystal Growth* **1970**, *6*, 210–212.
3. Amelinckx, S.; Maenhout-Van Der Vorst, M.; Dekeyser, W. Cavity Formation in Nitrate-Doped Alkali Halides. *Acta Metallurgica* **1959**, *7* (1), 8–17.
4. Borne, L.; Patedoye, J-C.; Spyckerelle, C. Quantitative Characterization of Internal Defects in RDX Crystals. *Propellants, Explosives, Pyrotechnics* **1999**, *24*, 255–259.
5. Batten, J. J. The Thermal Decomposition of RDX Below its Melting Point. *Australian Journal of Chemistry* **1972**, *25/11*, 2337–2351.
6. Sharma, J.; Coffey, C. S.; Armstrong, R. W.; Elban, W. L.; Lanzerotti, M.Y.D. Nanostructure of Porosity (and Entrapped Solvent Effects) in Laboratory-Grown Crystals of RDX as Revealed by an AFM. *AIP Conference Proceedings 505*, 2000, 719–722. DOI: 10.1063/1.1303574.
7. Bouma, R.H.B.; Duvalois, W.; Van Der Heijden, A.E.D.M. Microscopic Characterization of Defect Structure in RDX Crystals. *Journal of Microscopy* **2013**, *252/3*, 263–274. DOI: 10.1111/jmi.12088.
8. Stoltz, C. A.; Mason, B. P.; Hooper, J. Neutron Scattering Study of Internal Void Structure in RDX. *Journal of Applied Physics* **2010**, *107*, 103527/1-1-103527/6.
9. Ter Horst, J. H.; Geertman, R. M. ; van der Heijden A.E.D.M.; van Rosmalen, R. M. *Crystal Growth Rate and Impurity Effect During RDX Crystallization*, Proc. 30th Int. Annual Conference of ICT, 1999, paper 42.
10. Stoltz, C. A.; Mason, B. P.; Roberts, C. W.; Hira, S. M.; Strouse, G. F. Sonocrystallization as a Tool for Controlling Crystalline Explosive Morphology and Inclusion Content, Shock Compression of Condensed Matter – 2011. *AIP Conference Proceedings* 1426, 2012, 641-644. DOI: 10.1063/1.3686360.
11. Kim, D. Y.; Kim, K. J.; Kim, H. S. Semi-Quantitative Study on the Inclusion in Cooling Crystallization of RDX Using Various Solvents, Propellants. *Explos. Pyrotech.* **2010**, *35*, 38–45, DOI: 10.1002/prep.200800116.

12. Czerski, H.; Proud, W. G. Relationship Between the Morphology of Granular Cyclo Trimethylene–Trinitramine and its Shock Sensitivity. *Journal of Applied Physics* **2007**, *102*, 1–8.

13. Borne, L.; Beaucamp, A. Effects of Explosive Crystal Internal Defects on Projectile Impact Initiation, *12th Symposium (International) on Detonation*, 2002, 11 – 16.

14. Borne, L.; Ritter, H. HMX as an Impurity in RDX Particles: Effect on the Shock Sensitivity of Formulations Based on RDX, Propellants, Explosives. *Pyrotechnics* **2006**, *31* (6), 482–489.

15. Doherty, R. M.; Watt, D. S. Relationship between RDX properties and sensitivity. Propellants, Explosives. *Pyrotechnics* **2008**, *33* (1), 4–13.

16. Lochert, I. J.; Franson, M. D.; Hamshere, B. L. *Reduced Sensitivity RDX (RS-RDX) Part I: Literature Review and DSTO Evaluation*; DSTO-TR-1447, July 2003.

17. Wilson, W. S. *The Influence of Inert Particulate Material on the Properties of RDX/Polyethylene Wax Compositions*; MRL-R-929, May 1984.

18. Borne, L.; Mory, J.; Schlesser, F. Reduced Sensitivity RDX (RS-RDX) in Pressed Formulations: Respective Effects of Intra-Granular Pores, Extra-Granular Pores and Pore Sizes. Propellants. *Explosives, Pyrotechnics* **2008**, *33* (1), 37–43.

19. Addiss, J. W.; Proud, W. G. Relationship Between the Compaction Response and Morphology of RDX and Shock Sensitivity. Proc. New Trends in Research of Energetic Materials. *Proceedings of the 11th Seminar, NTREM*, Pardubice, Czech Republic, 2008, 40–51.

20. Zhang, W-B.; Tian, Y.; Yang, R-C.; Bin, D.; Yang, X-H. Characterization of Pressing Process of RDX Crystal Grain by Cone-beam Micro-focus Computed Tomography. *Proc. of the 18th World Conference on Nondestructive Testing*, Durban, South Africa, 2012, 16-20 .

21. Alexander, B. BAE Systems. Personal communication, 26 July 2012

22. Roos, B. D., ARL. Personal communication. 13 Dec 2012.

23. van der Heijden, A.E.D.M.; Bouma, R.H.B. Shock Sensitivity Of HMX/HTPB PBX's: Relation with HMX Crystal Density. *Proc. 29th Int. Annual Conference of ICT*, 1998, paper 65.

24. Waldschmidt, A.; Rietveld, I.; Couvrat, N.; Dupray, V.; Sanselme, M.; Berton, B.; Nicolai, B.; Mahé, N.; Petit, S.; Céolin, R.; Coquerel, G. About Aged Heterogeneous Liquid Inclusions Inside Organic Crystals in Relation to Crystal Formation, Structure, and Morphology. *Cryst. Growth Des.* **2011**, *11* (6), 2580–2587, DOI: 10.1021/cg200331n.

25. Shindo, I. The Growth Mechanism of Negative Crystals and Microscopic Point Imperfections in Flux Grown YAG Single Crystals. *Journal of Crystal Growth* **1981**, *51* (3), 573–580, DOI: 10.1016/0022-0248(81)90439-5.

26. Furukawa, Y.; Kohata, S. Temperature Dependence of the Growth Form of Negative Crystal in an Ice Single Crystal and Evaporation Kinetics for its Surfaces. *Journal of Crystal Growth* **1993**, *129* (3–4), 571–581, doi: 10.1016/0022-0248(93)90493-G.

27. Roedder, E. *Composition of Fluid Inclusions: Reviews of World Literature*, U.S. Government Printing Office, Washington, 1972.

28. Sorby, H.C. On the Microscopic Structure of Crystals, Indicating the Origin of Minerals and Rocks. *Quarterly Journal of the Geological Society*, London **1858**, *14*, 453–500. doi: 10.1144/GSL.JGS.1858.014.01-02.44.

29. Duan, X-H.; Liu C-J.; Qiao Y-L.; Zhou Y.; Nie F-D.; Pei, C-H.; Chen, J. Dendrite Growth of Energetic Material RDX. *Journal of Crystal Growth* **2012**, *351*, 56–61.

30. McGann, E. V.; Rothstein, L. R. *A Safety, Quality and Cost Effectiveness Study of Composition A-3*; NWSY TR 76-1, March 1976.

31. Military Explosives, Department Of The Army Technical Manual; Tm 9-1300-214, Headquarters, Department Of The Army, September 1984.

List of Symbols, Abbreviations, and Acronyms

AFM	atomic force microscopy
ARL	U.S. Army Research Laboratory
D	desorption
GC	gas chromatography
MREM	Multiscale Modeling of Energetic Material
MS	mass spectroscopy
NMR	nuclear magnetic resonance
RS-RDX	reduced-sensitivity RDX
SANS	small angle neutron scattering
SIC	selected ion chromatogram
TAX	1(N)-acetyl-3,5-dinitro-1,3,5-triazine
USANS	ultra small angle neutron scattering

1 DEFENSE TECHNICAL
(PDF INFORMATION CTR
only) DTIC OCA

1 DIRECTOR
(PDF) US ARMY RESEARCH LAB
RDRL CIO LL
IMAL HRA

1 GOVT PRNTG OFC
(PDF) A MALHOTRA

ABERDEEN PROVING GROUND

1 DIR USARL
(PDF) RDRL WML B
R PESCE-RODRIGUEZ

INTENTIONALLY LEFT BLANK.